

Virtual photoconductivity due to intense optical radiation transmitted through a semiconductor

Y. Yafet and E. Yablonovitch

Bell Communications Research, Navesink Research Center, Red Bank, New Jersey 07701-7040

(Received 18 July 1990)

Virtual photoconductivity is the change in static dielectric susceptibility due to the virtual excitation of electrons and holes by an optical beam in the transparent region of a semiconductor, near the band edge. It is the inverse of the Franz-Keldysh effect, which is the change in optical constants due to a strong static field. Previously, only the low-optical-intensity limit of virtual photoconductivity had been theoretically analyzed. We provide in this paper a nonlinear theory of virtual photoconductivity valid for strong optical fields. The main approximation is that the optical matrix element be strong enough to overwhelm the Coulomb interaction between electron and hole, but weak enough to avoid two-photon absorption. At high optical intensities, we find that the change of static dielectric constant saturates at ≈ 0.5 units. The saturated regime of virtual photoconductivity, while difficult to attain experimentally, is best explored on the red side of the exciton absorption tail in high-quality GaAs crystals at very low temperatures.

I. INTRODUCTION

There has been interest recently¹⁻³ in the change of static dielectric constant of a semiconductor caused by optical radiation at a frequency just below the band gap. When an optical beam propagates through a transparent semiconductor crystal, it induces a population of virtual electron-hole pairs which are readily polarizable by a static electric field. This change in dielectric constant has been called² "virtual photoconductivity" to distinguish it from the ordinary photoconductivity of real carriers produced by incident radiation in the absorbing region above the band gap.

Virtual photoconductivity is only one member of a general family of optoelectronic phenomena in which optical waves and static electric fields interact. In different contexts, these phenomena frequently have different names, but their physical origin is usually the same. For example, when an optical field changes the static (dc) dielectric constant it is sometimes described by a nonlinear susceptibility $\chi^{(3)}(0,0,-\omega_0,\omega_0)$, where ω_0 is an optical frequency, and the 0's represent a zero-frequency electric wave. In the context of bulk semiconductors, this is called virtual photoconductivity. In quantum wells, it is known as the ac-dc Stark effect.

Conversely, the same $\chi^{(3)}(-\omega_0,\omega_0,0,0)$, with variables permuted, tells us how a dc electric field changes the optical refractive index. This has been called electroreflectance,⁴ electrorefraction, or the quadratic electro-optic effect. But $\chi^{(3)}(-\omega_0,\omega_0,0,0)$ incorporates only the lowest-order term of a Taylor expansion in the dc field. In the limit of arbitrarily strong dc electric fields, this phenomenon becomes known as the Franz-Keldysh⁵ effect, and it includes electrically induced optical absorption, as well as refractive-index changes.

Thus we see that the influence of arbitrarily strong dc fields on the optical constants has been calculated and is well known.⁵ Furthermore, by permutation symmetry,

the effect of a weak optical field on the static dielectric constant, expressed by $\chi^{(3)}(0,0,-\omega_0,\omega_0)$, is also well known.² But to our knowledge, the influence of strong optical fields on the dc dielectric constant has never been calculated. In this paper we will present this virtual-photoconductivity effect in the limit of strong optical fields.

Naturally, the optical constants for frequencies ω_0 near the semiconductor band edge are particularly sensitive to a dc field perturbation. Conversely, an optical field at frequency ω_0 near the semiconductor band edge will produce an unusually large change in dc dielectric constant. This is an expression of the effect of virtual carriers. The closer the optical tuning to the band edge, the greater the population of virtual carriers, the stronger is their effect in screening the static dielectric constant. Once the optical frequency is above the semiconductor absorption edge, real carriers are created, and the physics becomes equivalent to conventional photoconductivity under intense light.

Our calculation neglects excitonic effects due to the electron-hole interaction. Inclusion of these effects at moderately high optical intensities is a very difficult problem, which we are not prepared to tackle. In the case of ordinary carriers, the effect of Coulomb interactions becomes negligible in the high-density limit. Likewise for virtual electron-hole pairs, excitonic interactions are negligible if the density is high due to a high optical intensity. The virtual-electron-hole-pair density can become larger than the reciprocal exciton volume if the optical matrix element becomes comparable to the detuning from the band edge. At the same time, two-photon absorption can remain negligible since it is nonresonant at the band edge. The main requirement is that the optical matrix element be strong enough to overwhelm the Coulomb interaction between electron and hole, but weak enough to avoid two-photon absorption.

II. OUTLINE OF CALCULATION

The effect of a static electric field on semiconductor band structure has an easy, exact, nonperturbative solution, as long as the electric field is below the limit where interband Zener tunneling becomes possible. This is sometimes called the acceleration theorem:⁶

$$\hbar \dot{k} = eE(0), \quad (1)$$

where k is the electron wave vector in the semiconductor band structure, e is the electronic charge, \hbar is Planck's constant divided by 2π , and $E(0)$ is the static electric field. This leads to a picture of the quantum states evolving in reciprocal space as $k \rightarrow k(t) = k + eE(0)t/\hbar$, which is exact for large electric fields subject to the restriction that Zener tunneling be negligible. An illustration of this type of temporal evolution in reciprocal space is given in Fig. 1(a).

To understand the effect of the dc field on the optical properties of the semiconductor, consider a pair of valence- and conduction-band states sharing the same position in k space. As they drift together in k space under the influence of the electric field, $k(t) \rightarrow k + eE(0)t/\hbar$, the energy spacing of the two states varies with time. As they approach the center of the Brillouin zone, the spac-

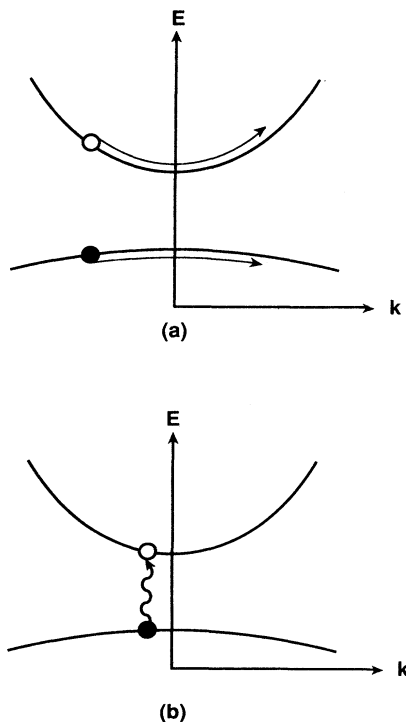


FIG. 1. A comparison of the time evolutions of the electronic wave functions in a direct-band-gap semiconductor, subject to (a) a strong static electric field, and (b) a strong optical field. Exact solutions exist in both cases. The optical spectrum of the first one leads to the Franz-Keldysh effect, while the static susceptibility of the second one leads to virtual photoconductivity.

ing can come as close as the band-gap energy. As they recede from the center of the Brillouin zone, the energy spacing becomes large again. To ask for the effect of a dc field on the optical spectrum is to ask for the linear optical spectrum of a two-level system subject to time-dependent energy spacing. In Eq. (1), the static problem is solved to all orders; and now the optical problem needs only to be solved to lowest order to determine the linear optical constants.

A time-varying energy spacing is a standard problem in spectroscopic line-shape theory. It has been solved in connection with nuclear magnetic resonance.⁷ There it gave rise to the idea of motional narrowing and other interesting changes in the linear, first-order, spectroscopic line shape. The essential trick is to Fourier transform the time-dependent phase factor as in line-shape theory, rather than simply doing a time average of the frequency-domain spectrum. That is in effect what Franz and Keldysh introduced⁵ when they calculated the effect of a static field on the optical spectrum. Their calculations found immediate application in studies of electroreflectance from semiconductors, where the surface depletion field significantly modifies the observed optical spectrum.

The problem of the present paper is the inverse problem, namely, the effect of an arbitrarily strong optical field on the static dielectric constant. The solution will follow the same pattern as above, except for treating optical and static fields in reverse order. First we determine a simple, exact solution valid for strong optical fields. Then we treat the static field as a weak perturbation on that time-dependent exact solution. We are fortunate that the two-band optical problem is exactly soluble to all orders, provided that we neglect other bands. In the optical-dipole approximation, the lattice periodicity of the crystal is maintained and the two-band system reduces to a collection of independent two-level systems indexed by the wave vector k . Two-level systems subject to a strong harmonic field are a classic textbook problem treated, for example, by Landau and Lifschitz⁸ or in the Feynman⁹ Lectures. It is also identical to the spin- $\frac{1}{2}$ problem in nuclear magnetic resonance. The exact optical solution is schematically illustrated in Fig. 1(b) to contrast it with the exact static field solution in Fig. 1(a).

With the exact optical solution in hand, we apply a weak static field perturbation $E(0)$. The induced electric-dipole moment gives us the static electric susceptibility, or the dielectric constant as a function of the optical intensity.

Our neglect of excitonic and other Coulomb effects means that our calculation is restricted to the case of strong optical fields. In the opposite limit, weak optical fields, excitonic and Coulombic effects are important and have been included in the treatment of bulk² virtual photoconductivity as well as in the ac-dc Stark effect in quantum wells.¹ Those weak-field results will be contrasted with the strong-field formulas in Sec. VII.

Schmitt-Rink, Chemla, and Miller have given³ an interesting descriptive analogy for the two opposite limits of weak and strong optical fields. They consider the weak-field limit as electron-hole *condensation in real*

space, due to the presumed importance of excitons; and the strong-field limit, electron-hole *condensation in momentum space*, due to the separation of the problem into independent two-level systems indexed by momentum wave vector k .

III. TWO-BAND MODEL IN AN OPTICAL FIELD

As outlined above, we want to find the exact solution to the problem of a semiconductor experiencing a strong optical field, i.e., we want to find the exact states of the Hamiltonian:

$$H_0(t) = \frac{1}{2m_0} \left[\mathbf{p} - \frac{e \mathbf{A}(t)}{c} \right]^2 + V_{\text{cryst}}, \quad (2)$$

where c is the speed of light, m_0 is the free-electron mass, and $\mathbf{A}(t)$ the vector potential of the optical field at a frequency ω_0 and polarization $\hat{\mathbf{x}}$,

$$\mathbf{A}(t) = [A(\omega_0)e^{i\omega_0 t} - A(-\omega_0)e^{-i\omega_0 t}] \hat{\mathbf{x}}. \quad (3)$$

In this paper, ω_0 will be smaller than the band gap ω_{cv} , but only slightly so, $\omega_{cv} - \omega_0 \ll \omega_0$. The amplitude $A(\omega_0)$ is chosen imaginary, which makes the electric field real, $E(\omega_0) = -i(\omega_0/c)A(\omega_0)$. The applied field is then $E(t) = 2E(\omega_0)\cos(\omega_0 t)$.

The electron states in the unperturbed crystal are

$$\Psi_m^0(r, t) = \Phi_m(r) e^{-i\omega_m t}, \quad (4)$$

where the index m takes on the values kc and kv for the conduction and valence bands, respectively. When an optical field is turned on adiabatically, these states evolve into linear combinations:

$$\Psi^\pm(r, t) = \sum_m a_m^\pm(t) \Psi_m^0(r, t) \quad (5)$$

where the superscripts $+$, $-$ label the states that evolved from the valence and conduction band, respectively. These superscripts will be dropped for the moment. The coefficients $a_m(t)$ are determined from the time-dependent Schrödinger equation. In Eq. (2), the term quadratic in $\mathbf{A}(t)$ does not depend on the electron variables and thus does not affect the electron states. Keeping only the linear term and writing

$$V(t) = -\frac{e}{m_0 c} \mathbf{p} \cdot \mathbf{A}(t) \quad (6)$$

we find in the usual way the equations for the $a_m(t)$,

$$i\hbar \frac{\partial a_m}{\partial t} = \sum_n V_{mn}(t) a_n, \quad (7)$$

where

$$V_{mn}(t) = e^{i(\omega_m - \omega_n)t} \langle \Phi_m(r) V(t) \Phi_n(r) \rangle. \quad (8)$$

At $k=0$, the momentum operator in Eq. (6) has only an interband matrix element, $n \neq m$. At $k \neq 0$, it has also diagonal matrix elements, $n = m$, which in fact are proportional to the group velocity of the carrier in that band and depend on odd powers of k . These matrix elements,

which reflect the loss of parity at $k \neq 0$ of the cell periodic functions $\Phi_m(r)$, are responsible for two-photon absorption in our model.¹⁰ Their direct effect on the wave functions is small because, being linear in k , they are small compared to the interband matrix element. We therefore neglect them and keep only the off-diagonal terms $m \neq n$ in Eq. (8). Since $\omega_{cv} - \omega_0 \ll \omega_0$, the rotating wave approximation is made. Letting $\omega_{cv}(k) \equiv \omega_c(k) - \omega_v(k)$, we define the k -dependent frequency $\varepsilon(k)$:

$$\varepsilon(k) \equiv \omega_{cv}(k) - \omega_0 = \varepsilon_0 + \frac{\hbar k^2}{2m_{\text{eff}}}, \quad (9)$$

where ε_0 is the detuning frequency from the band edge, $\varepsilon_0 \equiv \omega_{cv}(0) - \omega_0$, and m_{eff} is the reduced mass of the electron-hole excitation.

For small detuning, the change of the interband matrix element $\langle c | \mathbf{p} | v \rangle$ with k can be neglected, and Eq. (7) reduces to

$$i\dot{a}_c(t) = -q e^{i\varepsilon t} a_v(t), \quad (10a)$$

$$i\dot{a}_v(t) = -q e^{-i\varepsilon t} a_c(t), \quad (10b)$$

where the Rabi matrix element $\hbar q$ measures the interaction with the optical field:

$$\hbar q = -\frac{e}{m_0 c} p_{cv} \cdot A(\omega_0), \quad (11)$$

where q is the Rabi frequency and p_{cv} is the momentum matrix element at the band edge. We choose the phases of the Bloch functions such that p_{cv} is pure imaginary. Expressing p_{cv} in terms of the coordinate matrix element X_{cv} through the relation

$$p_{cv} = im_0 \omega_{cv} X_{cv} \quad (12)$$

and neglecting the difference between ω_0 and ω_{cv} , since they are nearly the same, we can express the Rabi matrix element $\hbar q$ in a physically more intuitive way as

$$\hbar q = e X_{cv} E(\omega_0), \quad (11')$$

where X_{cv} and $E(\omega_0)$ are real.

Equations (9a) and (9b) are solved by eliminating $a_v(t)$, which results in the equation

$$\ddot{a}_c - i\varepsilon \dot{a}_c + q^2 a_c = 0, \quad (13)$$

whose solutions are

$$a_c^\pm = e^{i\omega_\pm t}, \quad (14a)$$

$$a_v^\pm = \frac{\omega_\pm}{q} e^{-i\varepsilon t} a_c^\pm, \quad (14b)$$

where

$$\omega_\pm = \frac{\varepsilon}{2} \pm \left[\frac{\varepsilon^2}{4} + q^2 \right]^{1/2}. \quad (15)$$

The frequencies ω_\pm depend on the value of k through $\varepsilon = \varepsilon(k)$, Eq. (9). In the limit $q \rightarrow 0$, the solutions $[a_v^+(t), a_c^+(t)]$ and $[a_v^-(t), a_c^-(t)]$ reduce, respectively, to the unperturbed valence- and conduction-band states.

Making use of the relation $q^2 = -\omega_+ \omega_-$ which follows from Eq. (15), and defining

$$\alpha \equiv \frac{q}{\omega_+}, \quad (16)$$

we obtain the following expressions for the valence- and conduction-band states (corresponding to + and - above) in the presence of an optical field of arbitrary strength:

$$\Psi_{kv} = C e^{-i(\omega_v + \omega_-)t} [\Phi_{kv}(r) + \alpha \Phi_{kc}(r) e^{-i\omega_0 t}], \quad (17a)$$

$$\Psi_{kc} = C e^{-i(\omega_c - \omega_-)t} [\Phi_{kc}(r) - \alpha \Phi_{kv}(r) e^{i\omega_0 t}], \quad (17b)$$

where $C = (1 + \alpha^2)^{-1/2}$ is a normalization constant. Notice the frequency shifts occurring in the time exponentials of Eq. (17): They correspond to a repulsion in frequency (since ω_- is negative) between valence- and conduction-band states induced by the incident optical field.

IV. STATIC SUSCEPTIBILITY IN A STRONG OPTICAL FIELD

We now calculate the linear response of our system to a weak, static, uniform electric field. Initially the valence band is full and the conduction band is empty. The optical field is turned on adiabatically as $t \rightarrow -\infty$. The valence- and conduction-band states evolve into the states Ψ_{kv} and Ψ_{kc} of Eq. (17). These satisfy Schrödinger's equation:

$$i\hbar \frac{\partial \Psi_m}{\partial t} = H_0(t) \Psi_m, \quad (18)$$

where $H_0(t)$ is the time-dependent Hamiltonian of Eq. (2). A static electric field in the x direction gives rise to a perturbation $V' = -eE(0)x$ and the perturbed wave functions Ψ'_m satisfy

$$i\hbar \frac{\partial \Psi'_m}{\partial t} = [H_0(t) + V'] \Psi'_m, \quad (19)$$

where m again runs over kv and kc . The static susceptibility is obtained from the time-independent part of the expectation value of the dipole operator ex over the time-dependent states Ψ'_{kv} , calculated to first order¹¹ in $E(0)$.

It is easy to show, making use of Eq. (19), that the perturbed states Ψ'_m are found in the same way as when H_0 is time independent, namely, writing

$$\Psi'_n = \sum_m b_m(t) \Psi_m, \quad (20)$$

$$\frac{1}{\mathcal{V}E(0)} \langle ex \rangle_k \equiv \chi_k = \frac{2e^2}{\mathcal{V}\hbar(1+\alpha^2)^2} \left[\frac{(\partial\alpha/\partial k_x)^2}{(\epsilon^2 + 4q^2)^{1/2}} + \frac{|X_{cv}|^2}{(\epsilon^2 + 4q^2)^{1/2} + \omega_0} + \alpha^4 \frac{|X_{cv}|^2}{(\epsilon^2 + 4q^2)^{1/2} - \omega_0} \right]. \quad (28)$$

This then is the linear static susceptibility of a virtual electron-hole pair of wave vector k . The quantity $(\epsilon^2 + 4q^2)^{1/2}$ is familiar from magnetic-resonance work. Of the three terms in Eq. (28), the first is the most impor-

tant and we will discuss it in due course, but all three have simple physical interpretations.

$$i\hbar \frac{\partial b_m}{\partial t} = \sum_n V'_{mn} b_n \quad (21)$$

which are identical with Eq. (7).

To obtain Ψ'_{kv} to first order in $E(0)$ we take $b_{kv} = 1$, and from Eq. (21) obtain

$$b_{kc} = \frac{1}{i\hbar} \int_{-\infty}^t e^{\zeta t'} V'_{cv}(t') dt', \quad (22)$$

where ζ is a positive infinitesimal. Making use of Eq. (17) we find that

$$V'_{cv}(t) = C^2 e^{i(\omega_{cv} - 2\omega_-)t} \int d^3r (\Phi_{kc}^* - \alpha \Phi_{kv}^* e^{-i\omega_0 t}) \times [-eE(0)x] \times (\Phi_{kv} + \alpha \Phi_{kc} e^{-i\omega_0 t}). \quad (23)$$

A combination of frequencies appearing in the exponential time factor reduces to

$$\omega_{cv} - 2\omega_- - \omega_0 = (\epsilon^2 + 4q^2)^{1/2}. \quad (24)$$

In Eq. (23), the singular operator x acting on the product of $\alpha(k)$, a function of k , with a Bloch function, Φ_{kc} , gives

$$x\alpha(k)\Phi_{kc} = i \frac{\partial \alpha}{\partial k_x} \Phi_{kc} + \alpha(k) X_{vc} \Phi_{kv}, \quad (25)$$

where the matrix elements X_{vc} of the lattice-periodic operator X are given in Eq. (12). With use of Eqs. (24) and (25), we find that V'_{cv} is equal to

$$V'_{cv}(t) = -\frac{eE(0)}{1+\alpha^2} e^{i(\epsilon^2 + 4q^2)^{1/2}t} \times \left[i \frac{\partial \alpha}{\partial k_x} + X_{cv} e^{i\omega_0 t} - \alpha^2 X_{vc} e^{-i\omega_0 t} \right], \quad (26)$$

and the coefficient b_{kc} follows immediately from Eq. (22).

The expectation value of the dipole operator is finally

$$\langle ex \rangle_k = -\frac{2}{E(0)} \text{Re} [V'_{vc}(t) b_{kc}(t)], \quad (27)$$

where Re denotes the real part and $V'_{vc} = V'_{cv}^*$. From the expression, Eq. (26), for V'_{cv} it is seen that $\langle ex \rangle_k$ contains terms with frequencies 0, ω_0 , and $2\omega_0$. Separating out the static (0-frequency) part of $\langle ex \rangle_k$, and dividing by the applied electric field $E(0)$ and the normalization volume \mathcal{V} , we obtain

tant and we will discuss it in due course, but all three have simple physical interpretations.

The second term of Eq. (28) is simply the interband static susceptibility of a valence electron of wave number

k , modified by the repulsion between bands induced by the optical field. This repulsion leads to a decrease of the susceptibility with increasing $|E(\omega_0)|$.

The third term, proportional to α^4 , results from the interband matrix element X_{cv} taken between the admixture terms (second terms) of the wave functions in Eq. (17). It produces a change in susceptibility which is proportional to the optical intensity squared or $|E(\omega_0)|^4$. It is a three-photon absorption term (two optical photons and one zero-frequency photon), which becomes resonant for wave vectors k far away from the band edge at a resonant frequency,

$$\omega_r \simeq \frac{1}{2} \left[\omega_{cv}(k) + \frac{4q^2}{\omega_{cv}(k)} \right], \quad (29)$$

which is approximately one-half the electronic transition energy. Such a three-photon absorption has the character of a weak two-photon induced change in susceptibility. At exact resonance, $\omega_0 = \omega_r$, the contribution to the static susceptibility would be pure imaginary. It will tend to be a weak effect since the prefactor α^4 is very small and nonresonant. This effect is somewhat analogous to, and competes with, a dc current flow of free electrons and holes created by ordinary two-photon absorption, having the same power and spectral dependence. On the other hand, free electrons and holes can accumulate over a period of time and provide a substantial ordinary two-photon photoconductivity. This can be a serious competitor with virtual photoconductivity, which is the first term in Eq. (28) and the main point of this paper. We will have to examine, on a case-by-case basis, whether virtual photoconductivity or ordinary two-photon absorption induced photoconductivity is the dominant process.

The second and third terms of Eq. (28) were previously obtained by Schmitt-Rink, Chemla, and Haug,¹² though not in this form. Those authors were interested in the optical (as opposed to static) polarization induced by a weak optical probe field. Their Eq. (54) reduces to the sum of our second and third terms in the limit where the frequency ω_i of the test beam goes to zero. Our first term is not included in their result because they considered only the interband matrix element of the dipole moment.

We are interested in the static case, and so, in the following we concentrate on the first term of Eq. (28). This is a generalization to arbitrarily strong optical field of the perturbation result, Eq. (7) of Ref. 2. To see this, note that to lowest order in $E(\omega_0)$ the numerator, $(\partial\alpha/\partial k_x)^2$, reduces to

$$\left[\frac{\partial\alpha}{\partial k_x} \right]_{q \rightarrow 0}^2 = \left[\frac{eE(\omega_0)X_{cv}}{\hbar\epsilon} \right]^2 \frac{1}{\epsilon^2} \left[\frac{d\epsilon}{dk_x} \right]^2. \quad (30)$$

Identifying $\hbar\epsilon$ with $-W_{cv}$ in Ref. 13, and making use of identities (2.17a) and (2.17b) of that paper, and multiplying by 2 to sum over spin states, we obtain the integrand of Eq. (7) in Ref. 2:

$$\frac{e^2 |eX_{cv}|^2 \hbar^2}{2m_{\text{eff}} [E_{cv}(k) - i\Gamma - \hbar\omega_0]^4}, \quad (31)$$

where the phenomenological damping term Γ has been added, and $E_{cv} \equiv \hbar\omega_{cv}$.

Note that $\partial\alpha/\partial k_x$ vanishes at very strong fields. At any k value, if $q \gg \epsilon(k)$, the limiting value of $\partial\alpha/\partial k_x$ is

$$\left[\frac{\partial\alpha}{\partial k_x} \right]_{q \gg \epsilon} \sim -\frac{1}{2q} \frac{d\epsilon}{dk_x} \quad (32)$$

and as $q \rightarrow \infty$ the virtual-photoconductivity effect goes away. This seems contrary to physical intuition at first sight, but the following parallel makes this result understandable: As is clear from Eq. (28), virtual photoconductivity originates from the acceleration term of the coordinate x , and not from the regular interband part X_{cv} . If one applies an electric field to an insulator, the only contribution to the susceptibility arises from the interband part X_{cv} . The acceleration term $i(\partial/\partial k_x)$ causes all the filled states to move rigidly through the Brillouin zone, $k(t) \rightarrow k + eE(0)t/\hbar$, but this does not contribute to the susceptibility.

Now, in the limit of very large optical field, the valence- to conduction-band optical transition is saturated ($\alpha \rightarrow 1$ for $q \rightarrow \infty$). The degree of mixing does not change as k moves through the zone under the influence of $E(0)$ and the states move rigidly as if there were no optical intensity. Thus there is no contribution from the acceleration term to the susceptibility. In practice, of course, the applied optical field is never so large that, for all possible k , the Rabi frequency is greater than the detuning, $q \gg \epsilon(k)$. Thus there is always a contribution to the susceptibility, but we may expect it to peak at a finite value of Rabi frequency q .

The total susceptibility χ_s contributed by the first term of Eq. (28) is obtained by summing over states k and including a factor 2 for the electron spin. It is easily shown that

$$\frac{1}{1 + \alpha^2} \frac{\partial\alpha}{\partial k_x} = -\frac{q}{\epsilon^2 + 4q^2} \frac{d\epsilon}{dk_x} \quad (33)$$

so that

$$\chi_s = \frac{4e^2}{\hbar} \frac{1}{(2\pi)^3} \int d^3k \frac{q^2}{(\epsilon^2 + 4q^2)^{5/2}} \left[\frac{d\epsilon}{dk_x} \right]^2. \quad (34)$$

Although this integral can be handled as it is, we prefer to make a partial integration over k_x , making use of the zone periodicity of $\epsilon(k)$ to transform the integrand into an expression containing $d^2\epsilon/dk_x^2$ instead of $(d\epsilon/dk_x)^2$. This is achieved by using the relation

$$\int_{\text{BZ}} dk_x \frac{d}{dk_x} \left[f(\epsilon) \frac{d\epsilon}{dk_x} \right] = 0 \quad (35)$$

and setting

$$\frac{df}{d\epsilon} = \frac{1}{(\epsilon^2 + 4q^2)^{5/2}}. \quad (36)$$

Equation (34) becomes

$$\chi_s = \frac{e^2}{6\hbar q^2} \frac{1}{(2\pi)^3} \int d^3k \left[1 + \frac{1}{2} \left[\frac{\epsilon^2}{\epsilon^2 + 4q^2} \right]^{3/2} - \frac{3}{2} \left[\frac{\epsilon^2}{\epsilon^2 + 4q^2} \right]^{3/2} \right] \frac{d^2\epsilon}{dk_x^2} \quad (37)$$

which is also equal to

$$\chi_s = \frac{1}{3\pi^2} \frac{e^2}{m_{\text{eff}}} \int_0^\infty \frac{k^2 dk}{4q^2} \left[1 - \frac{\epsilon}{(\epsilon^2 + 4q^2)^{1/2}} - \frac{2q^2\epsilon}{(\epsilon^2 + 4q^2)^{3/2}} \right], \quad (38)$$

where the effective mass approximation has been made. (This approximation is good to within a few percent even for very strong optical fields.) Because ϵ depends on k quadratically, Eq. (38) is an elliptic integral. It has been calculated numerically; the result depends on the two parameters $\epsilon_0 \equiv \Delta/\hbar$, the detuning frequency with respect to the band edge, and $\eta \equiv q^2/\epsilon_0^2 \equiv |eX_{cv}E(\omega_0)/\Delta|^2$, a normalized intensity parameter which is the square of the ratio of the Rabi frequency to the detuning frequency from the band edge. Defining the dimensionless variable ξ through $\xi^2 = \hbar k^2/2m_{\text{eff}}\epsilon_0$, which measures the electron-hole pair kinetic energy in terms of the detuning, the result for χ_s is

$$\chi_s = \frac{2}{3\pi^2} \frac{e^2}{\hbar} \left[\frac{2m_{\text{eff}}}{\hbar\epsilon_0} \right]^{1/2} G(\eta) = \frac{4K_0}{3\pi^2} \left[\frac{E_b}{\Delta} \right]^{1/2} G(\eta) \quad (39)$$

where E_b is the exciton Rydberg binding energy, $K_0 \equiv 4\pi\chi_0$ is the ordinary static dielectric constant which appears in the exciton binding, and

$$G(\eta) = \int_0^\infty \frac{\xi^2 d\xi}{4\eta} \left[1 - \eta \frac{d}{d\eta} \right] \times \left[1 - \frac{1 + \xi^2}{[(1 + \xi^2)^2 + 4\eta]^{1/2}} \right]. \quad (40)$$

The calculated $G(\eta)$ is plotted in Fig. 2. It rises steeply near the origin, as $G(\eta) \sim (3\pi/64)\eta$, reaches a broad plateau with a maximum at optical intensity parameter $\eta \sim 4.4$, and then decreases very gradually.

V. MAGNITUDE OF VIRTUAL PHOTOCONDUCTIVITY

We confine the discussion of the applications of these results to GaAs. The relevant material parameters follow: reduced mass m_{eff} of the electron-hole pair is about $\sim 0.05 \times m_{\text{el}}$, the free-electron mass, the exciton binding energy $E_b \sim 4.2$ meV, the static dielectric constant $K_0 \approx 13$, and the band-to-band electric dipole matrix element $X_{cv} \approx 7$ Å. Then the optically induced static susceptibility χ_s , which is a function of normalized optical intensity η , and detuning energy Δ is

$$\chi_s(\Delta, \eta) = \left[\frac{11 \text{ meV}}{\Delta} \right]^{1/2} G(\eta). \quad (41)$$

For the value $\Delta = 12$ meV used in Ref. 2, and at an optical intensity parameter $\eta = 1$, we find from Fig. 2 that the optically induced change in static susceptibility is $\chi_s = 0.037$ and the change in dielectric constant $K_s \equiv 4\pi\chi_s = 0.46$. This is substantially smaller than the linear extrapolation employed in Ref. 2, and the reason is evident from Fig. 2. There is already substantial non-linear saturation of the virtual photoconductivity at $\eta < 1$. For the same detuning, the maximum value of the change in dielectric constant K_s , reached at an intensity $\eta = 4.4$, is $(K_s)_{\text{max}} = 0.57$. Comparing K_s to the background static susceptibility, K_0 , this is a $\sim 5\%$ increase.

To understand why the virtual photoconductivity is not any larger, we first notice, from Eq. (28) that χ_s originates from the acceleration term in the interaction, while the background static susceptibility χ_0 originates from the interband term X_{cv} , which is large in semiconductors. It nevertheless would seem that the small denominator $(\epsilon^2 + 4q^2)^{5/2}$ in Eq. (34), which reduces to ϵ^5 at $q \rightarrow 0$, would give a large enhancement at small detuning and thus lead to a substantial effect. However, this denominator is small only over a small region of k space near the direct gap. For larger energies the fifth power dependence actually makes for a rapid increase of the denominator, and so most of k space contributes very little to χ_s .

In addition $(\epsilon^2 + 4q^2)^{5/2}$ increases rapidly with q , which measures the optical field amplitude. This increase

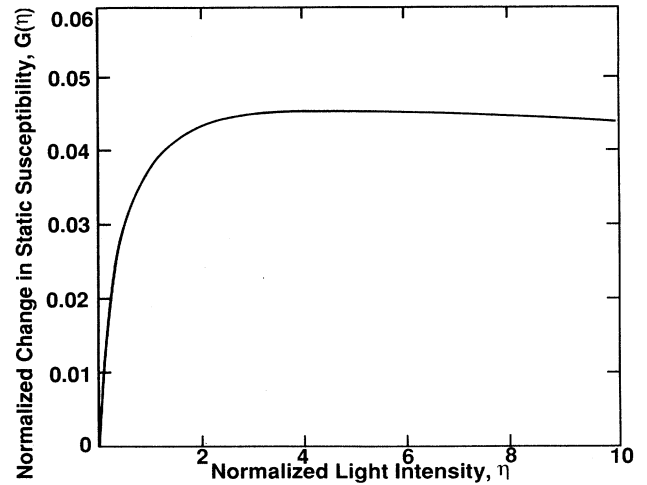


FIG. 2. The change in static susceptibility (virtual photoconductivity), in bulk material is linearly proportional to $G(\eta)$ according to Eq. (39), where η is the dimensionless optical intensity. Here η is the square of the ratio of Rabi frequency (or optical matrix element) to detuning frequency Δ from the band edge. At a detuning $\Delta = 10$ meV, $\eta = 1$ at 380 MW/cm². The peak change in the dielectric constant occurs at an intensity $\eta \approx 4.4$ and is $(K_s)_{\text{max}} \approx 0.5$.

causes $G(\eta)$ to level off even as the optical intensity parameter η approaches 2. That is why extrapolating the perturbation result to $\eta \approx 1$ substantially overestimates the saturated change in dielectric constant.

So far we have neglected the contributions of the second and third terms of Eq. (28). Both lead to a decrease in the real part of the susceptibility with increasing q , while the third term contributes, in addition, an imaginary part. In the range of values of Δ and η of interest here, both contributions can be neglected and we must consider, instead, two-photon induced photoconductivity as the most serious parasitic effect. Two-photon absorption does not appear in our formalism; as discussed after Eq. (8) it is left out of our calculation. Away from the band edge in GaAs, the s and p wave functions change their symmetry, and two-photon absorption becomes allowed. We will discuss it and other parasitic effects in the experimental feasibility section at the end of this paper.

We should also reiterate at this point our key approximation of neglecting Coulombic interactions by the virtual electrons and holes. At high intensities, the main regime of this paper, such interactions tend to be much weaker than the Rabi energy, $\hbar q$, and were therefore neglected. But at low intensities such effects play a role. In our previous paper on this subject, Ref. 2, which concentrated on the low-optical-intensity limit, we tried to incorporate Coulomb effects by expressing the final results in terms of the empirical optical-absorption spectrum. The empirical spectrum obviously contains Coulomb interactions. Thus Eqs. (8)–(12) of Ref. 2 are expressed in terms¹⁴ of the empirical interband optical-absorption spectrum. In addition, the sharp exciton line of the absorption spectrum was given special handling in Eq. (12) of Ref. 2. At low optical intensity Coulomb effects tend to enhance virtual photoconductivity, and this is partly responsible for the overestimate inherent in the linear extrapolation to higher intensity. Conversely, the low intensity limit of our Eqs. (37)–(41) should not be expected to agree exactly with the equations given in Ref. 2. They are meant to be used at high intensities. *Under weak optical pumping use the virtual-photoconductivity formulas given in Ref. 2.*

Among the important Coulomb interactions which are absent at our level of approximations is Coulomb damping, or simply electron-hole collisions. In our formalism such damping would produce an imaginary component to the susceptibility change χ_s . This would allow real absorptive transitions, as well as purely reactive virtual interband transitions, to occur. After the passage of the laser pulse, not all the virtual electrons would return to the valence band, as required for a purely reactive process. The virtual photoconductivity would have to compete with ordinary one-photon interband photoconductivity. A strong Rabi energy $\hbar q$ would tend to force a reversible adiabatic change. It is clear therefore that the use of the ordinary linear absorption coefficient would overestimate dissipative absorption. In the absence of any better theoretical model, the linear absorption formula would be a simple, worst-case bound for assessing the importance of nonadiabatic, absorptive, interband photoconductivity. Experimental feasibility for the observa-

tion of virtual photoconductivity in the presence of competing processes will be reviewed in the final section of this paper.

VI. VIRTUAL PHOTOCONDUCTIVITY IN QUANTUM WELLS

In view of the current interest in quantum confined systems and heterostructures we now discuss two-dimensional (2D) systems. Let us denote the susceptibility change by $\chi_s(2D)$ to distinguish it from the 3D case. We will analyze only the case of static electric field in the plane x - y of the layer. (The perpendicular dc field case was already handled in Ref. 1, and it leads to weaker effects since the polarization of the virtual electrons and holes is limited by the walls of the quantum well.) We find that for thin quantum wells $\chi_s(2D)$ can be slightly larger than its 3D counterpart χ_s .

We proceed from Eq. (37). In two dimensions the sum over electron states per unit volume is

$$\frac{1}{L^2 \tau} \sum_{k_x, k_y, k_z} = \frac{1}{(2\pi)^2} \frac{1}{\tau} \sum_{k_z} \int dk_x \int dk_y, \quad (42)$$

where L^2 is the area of the layer and τ its thickness. Summing over k_z adds the contributions of the subbands n . In each subband $dk_x dk_y = 2\pi(m_{\text{eff}}/\hbar)d\epsilon'$, where ϵ' is the frequency associated with the kinetic energy at k_x and k_y . The detuning, defined with respect to the energy at $k_x = k_y = 0$, is now different for each subband. Thus the detuning of the lowest subband is $\epsilon_0(1) = \omega_{cv}(0) - \omega_0 + (\hbar/2m_{\text{eff}})(\pi/\tau)^2$, while that of the higher subbands is $\epsilon_0(n) = \epsilon_0(1) + (n^2 - 1)(\hbar/2m_{\text{eff}})(\pi/\tau)^2$. This rapid increase of $\epsilon_0(n)$ with n assures a rapid convergence in the summation over n .

For each n , the quantity ϵ in Eq. (37) is $\epsilon = \epsilon_0 + \epsilon'$. Integrating Eq. (37) over ϵ' gives the result

$$\chi_s(2D) = \frac{1}{3\pi} \frac{e^2}{\tau \hbar} \sum_{n=1}^{\infty} \frac{1}{\epsilon_0(n)} F(\eta_n), \quad (43)$$

where $\eta_n = q^2[\epsilon_0(n)]^2$. The function $F(\eta)$ is

$$F(\eta) = \frac{1}{4\eta} \left[\frac{1+2\eta}{(1+4\eta)^{1/2}} - 1 \right]. \quad (44)$$

This is plotted in Fig. 3, and it is seen to be fairly similar to $G(\eta)$. It rises with an initial slope $F(\eta) \sim \eta/2$. The ratio of $\chi_s(2D)$ to χ_s is obtained from Eqs. (39) and (43); keeping only the first term in the sum, this is

$$\frac{\chi_s(2D)}{\chi_s} = \frac{1}{2} \left[\frac{\hbar^2 \pi^2}{2m_{\text{eff}} \tau^2} \frac{1}{\hbar \epsilon_0(1)} \right]^{1/2} \frac{F(\eta)}{G(\eta)} \quad (45)$$

and at any given value of η , it is determined by the square root of the ratio of confinement energy to detuning energy. For GaAs at a detuning $\Delta = 12$ meV, the confinement energy equals Δ for a thickness $\tau = 270$ Å. For $\eta = 1$, the ratio $\chi_s(2D)/\chi_s$ equals 1.5. For a thickness half of that, $\tau = 135$ Å, the ratio becomes 2.3. These are not very large ratios but they are somewhat interesting.

It is instructive to compare the behaviors of the functions $F(\eta)$ and $G(\eta)$. From Figs. 2 and 3 we notice that

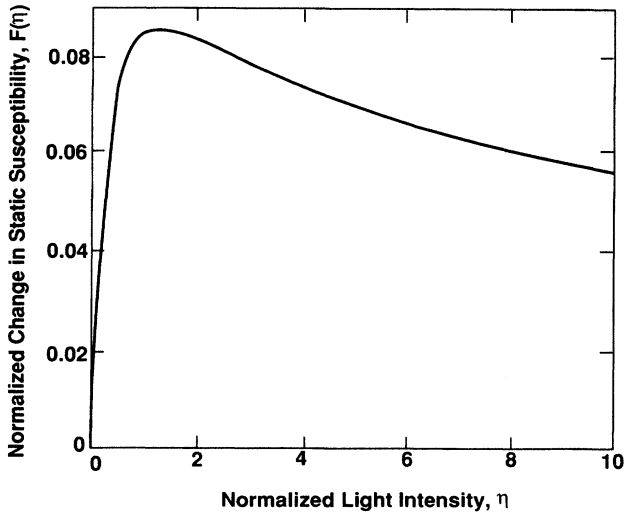


FIG. 3. The change in static susceptibility contributed by the lowest subband of a multiple-quantum-well structure is proportional to $F(\eta)$. The static field is assumed parallel to the layers. As in Fig. 2, η , the dimensionless optical intensity, is the square of the ratio of Rabi frequency (or optical matrix element) to detuning frequency Δ from the lowest subband edge.

$F(\eta)$ rises more steeply than $G(\eta)$ near the origin (both are linear in η) but, having reached its maximum $F(\eta)$ then decreases more rapidly than $G(\eta)$ as η continues to increase. This can be understood as a combination of two factors.

(1) In a given subband (and in the effective mass approximation) the 2D density of states compared to the 3D density of states is larger at small k_{\parallel} . The crossover point is in fact at $k_{\parallel} = \pi/\tau$, at which value the kinetic energy in the x - y plane equals the confinement energy.

(2) The integrand $f(\epsilon, q)$ in Eq. (37) is largest at $k = 0$ and decreases with increasing ϵ at any fixed q (or η). However, this decrease is more pronounced near $k_{\parallel} = 0$, the smaller the value of η [f varies as $(q/\epsilon)^4$ when $\eta \rightarrow 0$]. At larger values, $\eta \gtrsim 1$, the integrand is fairly constant over regions of k_{\parallel} space where $k_{\parallel} \gtrsim (\pi/\tau)$. Because the 2D density of states weights the integrand at small values of k_{\parallel} more heavily, the integral in the 2D case is more sharply peaked around its maximum than in the 3D case. We mention in passing that the rectangular state density of the 2D case resembles closely the approximation we made in Ref. 2 for treating Coulomb effects in the low-optical-intensity limit.

VII. EXPERIMENTAL FEASIBILITY

Considering how conceptually straightforward virtual photoconductivity actually is, we wonder why it has not yet been observed. Optics, and nonlinear optics in particular, have achieved by now a high level of sophistication and many more subtle effects have already been experimentally explored. To answer these questions, let us first

take note of the requirement for a high-power laser beam that is tuned almost to the absorption edge of a direct-band-gap semiconductor. A number of competing effects exist which could mask the virtual photoconductivity. In this section we will analyze this competition and see how to design an effective experiment.

With regard to the high-power requirements, let us ask what optical intensity is required to make $\eta \equiv q^2/\epsilon_0^2 \equiv |eX_{cv}E(\omega_0)/\Delta|^2 = 1$ at a typical detuning, say $\Delta = 10$ meV. Using a band-to-band dipole matrix element $X_{cv} = 7$ Å, the electric field requirement is $E(\omega_0) = 1.43 \times 10^5$ V/cm. The optical intensity is $cn|E(\omega_0)|^2/2\pi$, where n is the optical refractive index, $n \sim 3.5$. This leads to a requirement for 380 MW/cm², which, while substantial, amounts to $\ll 1$ mJ/cm² in a subpicosecond pulse. Furthermore, as can be seen from Fig. 2, much of the power above $\eta = 0.5$ is wasted due to saturation of the virtual-photoconductivity effect. Thus an intensity ~ 190 MW/cm² could produce almost the same effect.

By far the most serious parasitic effect is ordinary photoconductivity due to the real, as opposed to virtual, excitation of electrons and holes. This ordinary photoconductivity could be the result of one-photon absorption or two-photon absorption. Neither effect was included in our theory because (1) nonresonant one-photon absorption would require a Coulomb damping or other carrier collisions to produce a finite linewidth. The theory of the Urbach edge line shape is notoriously difficult, even in linear optics. (2) Two-photon absorption was excluded as explained after Eq. (8).

To analyze the competition between a static susceptibility change as against a photocurrent density, note that $\partial P/\partial t$ plays the same role as electrical current J in Maxwell's equations. Therefore the photocurrent $Ne\mu E(0)$ (in esu) should be compared against $(\partial\chi_s/\partial t)E(0)$, where N is the photocarrier density and μ the mobility of the carriers and $E(0)$ is the static bias field as always. One of the best ways of detecting such high speed currents is to use them to generate¹⁵ microwave or millimeter wave pulses, much as Hertz did with radio waves 100 years ago. Then the microwave radiated power is proportional to the square of the source terms, $\partial J/\partial t$ in one case, and $\partial^2 P/\partial t^2$ in the other case. Hertzian radiation is superior to a simple current measurement in a conventional photodiode, since it discriminates against long-lived real carriers which continue to flow in a photodiode long after the laser pulse has gone.

Therefore we need to compare $\partial^2\chi_s/\partial t^2$ against $e\mu\partial N/\partial t$. Since carrier lifetimes are generally very long in good quality semiconductors, the photocarrier density N is the time integral $\int dt M[\eta(t)]$, over the real carrier generation rate per unit volume M , which is a function of the dimensionless intensity $\eta(t)$. For linear absorption $M[\eta]$ is linear, and for two-photon absorption $M[\eta]$ is quadratic. Now the comparison is between $\partial^2\chi_s/\partial t^2$ as against $e\mu(\partial/\partial t)\int dt M[\eta(t)]$ which in turn simplifies nicely to $e\mu M[\eta(t)]$.

Using the information in this paper it is easy to estimate $\partial^2\chi_s/\partial t^2$ which can be written χ_s/T^2 , where T is a

characteristic time which for most laser pulse shapes is approximately one-half the laser pulse duration. An average detuning of $\Delta = 10$ meV allows sufficient bandwidth for a laser pulse ~ 0.12 psec in duration. Then for the change $\chi_s \approx 0.039$, the source term of Hertzian radiation becomes $\partial^2 \chi_s / \partial t^2 \approx 1.08 \times 10^{25} / \text{sec}^2$. This has to be compared against the ordinary photoconductive source term, $e\mu M[\eta(t)]$, first for linear absorption, and then for two-photon absorption.

In respect of the fact that the photoexcited carriers in GaAs are likely to be quite energetic, let us employ a carrier mobility $\mu \sim 5000$ cm²/V sec, which must be multiplied by 300 to convert to esu. The shape of the Urbach edge in GaAs is known¹⁶ at 75 K and it is evident that it must be even sharper at lower temperatures. At 4 K an absorption coefficient $< 1/\text{cm}$ seems entirely reasonable for a detuning of only 10 meV. Then the Hertzian source term caused by linear absorption induced carriers is

$$e\mu \times (1 \text{ cm}^{-1}) \times \frac{380 \text{ MW cm}^{-2}}{\hbar\omega_{cv}} = 1.22 \times 10^{24} \text{ sec}^{-2}. \quad (46)$$

This is safely less than the virtual source term $\partial^2 \chi_s / \partial t^2 \approx 1.08 \times 10^{25} / \text{sec}^2$.

Now let us consider two-photon transitions whose absorption coefficient¹⁷ in GaAs is $\beta = 2.6 \times 10^{-8}$ cm W⁻¹. The Hertzian source term associated with two-photon induced carriers is

$$e\mu\beta \frac{(380 \text{ MW cm}^{-2})^2}{\hbar\omega_{cv}} = 1.2 \times 10^{25} \text{ sec}^{-2} \quad (47)$$

which is marginally larger than the virtual source term $\partial^2 \chi_s / \partial t^2 \approx 1.08 \times 10^{25} / \text{sec}^2$. In the attempt to reach the fully saturated regime of virtual photoconductivity, the optical intensity has become high enough to cause comparable two-photon photoconductivity. To examine the tradeoffs between the competing photoconductivities, let us write down the following scaling laws for optical field, and the Hertzian source terms for virtual, linear, and two-photon photoconductivity in the saturated regime where the dimensionless intensity $\eta \sim 1$:

$$|E(\omega_0)| \sim \Delta, \quad (48a)$$

$$\partial^2 \chi_s / \partial t^2 \sim \Delta^{3/2}, \quad (48b)$$

$$\text{linear photoconductivity} \sim \Delta^2, \quad (48c)$$

$$\text{two-photon photoconductivity} \sim \Delta^4. \quad (48d)$$

A thoughtful examination of these scaling laws tells us that the saturated regime of virtual photoconductivity demands the smallest possible detuning, Δ , if it is to dominate the other photoconductivities. This in turn requires the best possible material quality and the sharpest, cleanest, exciton Urbach tail. A detuning of 10 meV permits the two-photon photoconductive signal to be competitive with the virtual photoconductivity. Clearly it is desirable to work even closer, right at the red edge of the bulk exciton, but before significant linear absorption sets in. Unfortunately, the absolute strength of the band-tail

absorption in GaAs below¹⁶ 75 K appears not to be available in the literature.

The plethora of photoconductive signals can still be distinguished from one another, even when they are of similar strength. The ordinary photoconductivity produces a Hertzian source term that is always positive, but the virtual source term is a second derivative with two zero crossings. These added zero crossings will show up in the coherently¹⁵ detected microwaves.

It is interesting to analyze whether there is any prospect of detecting virtual photoconductivity at room temperature. The slope of the Urbach edge is much less steep at room temperature. A detuning of at least 50 meV is needed, dashing any hopes of reaching the $\eta = 1$ saturated regime. From Ref. 2, the virtual photoconductivity is proportional to $\sim \Delta^{-3}$, and the signal will be weaker by $5^3 = 125$ compared to the 10-meV detuning we analyzed above. Since the two-photon contribution does not fall off away from the band edge, the peak power will have to be reduced by a factor 125 to keep pace. Therefore the optimal optical intensity for detecting the virtual photoconductivity at room temperature would be only ~ 1 MW/cm². It is impossible to reach the saturation limit of Figs. 2 and 3 at room temperature.

At low intensity the only competing process is ordinary linear photoconductivity. Since Urbach tails fall away exponentially with detuning Δ from the band edge, and virtual photoconductivity falls away as the reciprocal cube of the detuning, the virtual photoconductivity will always dominate ordinary photoconductivity at sufficiently large detuning as required at room temperature. But then the effect is considerably weakened in comparison to the saturated condition. At a 5 times greater detuning, and 125 times less power as specified in the preceding paragraph, the change in dielectric constant is weaker by $\sim 10^5$. But the volume integrated Hertzian source term is not necessarily that much smaller since it is not confined to the optical skin depth. We conclude that virtual photoconductivity at room temperature is within the signal-to-noise capabilities of current laser-microwave photoconductivity experiments.

One more parasitic electro-optic effect needs to be dispensed with, and that is optical rectification. It is the inverse of the linear electro-optic effect. In optical rectification, the passage of an optical beam through an inversion nonsymmetric semiconductor sets up a static polarization. It is nonresonant at the band edge, so at small detuning the virtual photoconductivity will always win. In GaAs the linear electro-optic coefficient¹⁸ is $r_{xyz} \approx 4.8 \times 10^{-8}$ esu. At some finite static bias field, virtual photoconductivity will become competitive with the static polarization of the optical rectification effect. We find that this would require a static field $E(0) > 10^4$ V/cm at a detuning $\Delta = 50$ meV. One has the option of applying a bias field stronger than this to overwhelm the optical rectification effect. Alternatively, taking advantage of the xyz symmetry of the optical rectification coefficient, it is eliminated when the optical polarization is along one of the cubic axes.

We are now in a position to answer why virtual photoconductivity has not yet been experimentally observed in

subpicosecond spectroscopy. At the large detunings required at room temperature, the effect is rather weak, though still detectable by microwave or millimeter wave generation. In fact it is the dominant photoconductivity at detunings > 50 meV. Direct detection by current flow in a photodiode is inadvisable since there is no way to discriminate against the long-lived real current flows of ordinary photoconductivity. At low temperatures, ≈ 4 K, the effect can be much larger, almost saturated, but it requires extremely good material quality. Then the optimal laser tuning would be just on the red edge of the bulk exciton absorption tail. The outlook is promising for virtual photoconductivity to be observed experimentally.

VIII. CONCLUSIONS

We have analyzed the saturation of virtual photoconductivity as a function of optical intensity. The saturation requires an intensity sufficient to make the optical

transition matrix element equal to the detuning energy. The change in dielectric constant saturates at a change of $(K_s)_{\max} \approx 0.5$. To achieve such a large change in dielectric constant, and to minimize competing effects, requires a very cold semiconductor crystal of the highest possible quality. The laser pulse should be tuned as close to the red edge of the bulk exciton as permitted by the laser pulse bandwidth and the absorption tail.

A multiple-quantum-well structure (MQWS) would have only a marginally stronger virtual photoconductivity than bulk material. A static bias field parallel to the plane of the quantum wells is preferable to perpendicular. The advantages of the MQWS would probably be outweighed by the limited volume filling fraction, and by the better quality of bulk material. Furthermore, the Urbach tail of the bulk exciton is likely to be sharper since it is not subject to quantum-well thickness fluctuations. In addition, bulk excitation would give a bigger signal since a larger volume of material would be likely to be excited and to radiate a microwave signal.

¹D. S. Chemla, D. A. B. Miller, and S. Schmitt-Rink, *Phys. Rev. Lett.* **59**, 1018 (1987).

²E. Yablonovitch, J. P. Heritage, D. E. Aspnes, and Y. Yafet, *Phys. Rev. Lett.* **63**, 976 (1989); **63**, 1896(E) (1989).

³S. Schmitt-Rink, D. S. Chemla, and D. A. B. Miller, *Adv. Phys.* **38**, 89 (1989).

⁴D. E. Aspnes, *Surf. Sci.* **37**, 418 (1973).

⁵W. Franz, *Z. Naturforsch.* **13a**, 484 (1958); L. V. Keldysh, *Zh. Eksp. Teor. Fiz.* **34**, 1138 (1958) [*Sov. Phys.—JETP* **7**, 788 (1958)].

⁶W. V. Houston, *Phys. Rev.* **57**, 184 (1940); C. Kittel, *Quantum Theory of Solids* (Wiley, New York, 1963), see p. 190.

⁷N. Bloembergen, *Nuclear Magnetic Relaxation* (Benjamin, New York, 1964).

⁸L. Landau and E. M. Lifschitz, *Quantum Mechanics, Non-relativistic Theory* (Pergamon, London, 1958), see p. 143.

⁹R. P. Feynman, R. B. Leighton, and M. Sands, *The Feynman Lectures on Physics* (Addison-Wesley, New York, 1965), Vol. III.

¹⁰H. J. Fossum and D. B. Chang, *Phys. Rev. B* **8**, 2842 (1973).

¹¹Actually the dipole operator has a nonvanishing expectation

value even in the wave functions Ψ_{kv} that are zero order in $E(0)$. However, it is clear from Eq. (25) that the in-band part of x , which is $i\partial/\partial k_x$, gives a time-independent contribution that is odd in k_x so that the sum over k vanishes. The inter-band part X_{cv} gives only a contribution at frequency ω_0 , i.e., no static dipole moment.

¹²S. Schmitt-Rink, D. S. Chemla, and H. Haug, *Phys. Rev. B* **37**, 941 (1988).

¹³D. E. Aspnes and J. E. Rowe, *Phys. Rev. B* **5**, 4022 (1972).

¹⁴Equation (9) of Ref. 2 is too low by a factor $\frac{3}{4}$ due to a numerical error. See E. Yablonovitch, J. P. Heritage, D. E. Aspnes, and Y. Yafet, *Phys. Rev. Lett.* **63**, 1896(E) (1989).

¹⁵X.-C. Zhang, B. B. Hu, J. T. Darrow, and D. H. Auston, *Appl. Phys. Lett.* **56**, 1011 (1990).

¹⁶A. Von Lehman, J. E. Zucker, J. P. Heritage, and D. S. Chemla, *Phys. Rev. B* **35**, 6479 (1987).

¹⁷J. S. Aitchison, M. K. Oliver, E. Kapon, E. Colas, and P. W. E. Smith, *Appl. Phys. Lett.* **56**, 1305 (1990).

¹⁸A. Yariv, *Optical Electronics*, 3rd ed. (Holt, Rinehart and Winston, New York, 1985), see p. 280.